

Carbon nanotube-based neat fibers

Macroscopic fibers containing only Carbon NanoTubes (CNTs) will yield great advances in high-tech applications if they can attain a significant portion of the extraordinary mechanical and electrical properties of individual CNTs. Doing so will require that the CNTs in the fiber are sufficiently long, highly aligned and packed in an arrangement that is nearly free of defects. Here we review and compare the various methods for processing CNTs into neat fibers. These techniques may be divided into 'liquid' methods, where CNTs are dispersed into a liquid and solution-spun into fibers, and 'solid' methods, where CNTs are directly spun into ropes or yarns. Currently, these processes yield fibers whose properties are not sufficiently close to optimal; however, the last five years have seen rapid progress, and the production of commercially useful CNT fibers may be achieved in the next few years.

Natnael Behabtu^{a,b}, Micah J. Green^{a,b}, and Matteo Pasquali^{a-c *}

^aDepartment of Chemical and Biomolecular Engineering, MS-362, Rice University, 6100 Main Street, Houston, TX 77005, USA

^bThe Smalley Institute for Nanoscale Science & Technology, Rice University, 6100 Main Street, Houston, TX 77005, USA

^cDepartment of Chemistry, Rice University, 6100 Main Street, Houston, TX 77005, USA

*E-mail: mp@rice.edu

The discovery and subsequent development of new materials are often the catalyst for technological breakthroughs, particularly when a qualitative leap in electrical, thermal or mechanical properties occurs. The field of fiber applications is poised for such a breakthrough. In the past 50 years, fibers composed of rod-like polymers have had a great impact on aerospace, military and industrial applications requiring lightweight, mechanically strong materials¹. Carbon NanoTubes (CNTs) have a rod-like geometry and high molecular stiffness²⁻⁴, similar to rod-like polymers and they possess a unique combination of excellent

mechanical, thermal and electrical properties. Single-Walled carbon NanoTubes (SWNTs) and MultiWalled carbon NanoTubes (MWNTs) are effectively rolled-up graphene sheets and share the exceptional mechanical properties of graphene (modulus and tensile strength)⁵. Experiments indicate an average modulus of 1 TPa and tensile strength of 13-53 GPa for SWNTs; these values are virtually independent of diameter. The electrical conductivity and current-carrying capacity of 'armchair' SWNTs exceed those of Cu and their thermal conductivity is higher than that of diamond⁶⁻⁸. Fibers composed of such CNTs have the potential to form high-

strength, lightweight, thermally and electrically conducting materials⁸. However, a number of hurdles must be overcome in order to realize this potential, including the difficulty of processing CNTs into a macroscopic article that retains enough of the properties of the constituent CNTs.

The method of CNT production strongly influences the type (MWNT vs. SWNT), length (submicron to millimeter), chirality, and processability, which in turn determines the properties of the final CNT-based macroscopic product. Here we briefly describe the various means of synthesizing CNTs and review the various approaches used for neat fiber production.

Nanotube synthesis

Research on CNT synthesis and research on CNT fibers are interdependent, with fibers and other applications driving new discoveries in CNT catalysis and growth. Many of the key advances in CNT synthesis led immediately to new results in fiber production. Below we review various synthesis techniques which can produce either shorter nanotubes (including arc-discharge, laser oven, high-pressure CO conversion (HiPco), fluidized bed Chemical Vapor Deposition (CVD)) or longer nanotubes (substrate growth CVD, catalytic gas flow CVD).

Systematic research into CNTs began with Iijima's⁹ observation of MWNTs produced in an arc-discharge fullerene reactor. Gram-level production was attained rapidly¹⁰. SWNTs were discovered soon after through the use of metal catalysts in an arc-discharge system¹¹. The properties of individual SWNTs are even more promising than those of MWNTs, particularly in regard to electrical and optical properties. Milligram-level quantities of SWNTs were produced by adapting laser ablation, a technique used to produce fullerenes¹², to attain a high yield (>70%) of defect-free SWNTs (~1.4 nm diameter)^{13,14}. A laser beam evaporates a graphite sample containing 1% Ni and Co catalyst particles; in the resulting vapor, the metal aggregates into C-saturated catalyst nanoparticles, from which sprout SWNTs. These catalyst particles are necessary to produce SWNTs rather than MWNTs¹⁵. A gas-phase CVD process, termed HiPco, was developed¹⁶; this process is both cheaper and more scalable, partly because it does not use preformed catalyst particles, unlike alternative CVD processes for SWNTs.

These alternative CVD processes involve the formation of CNTs on preformed metal nanoparticles which catalyze the decomposition of a gaseous C compound and subsequent growth of either SWNTs or MWNTs¹⁷. Different C precursors can be used, including CH₄, CO, alcohols, and acetylene. These alternative CVD processes are attractive because the reaction temperatures can be ~400 K lower than the arc discharge and laser ablation techniques. Several different CVD methods have been used, including fluidized bed¹⁸, substrate growth^{19–21} and 'catalytic gas flow CVD'^{22,23}. Fluidized bed CVD, along with laser oven, arc discharge and HiPco methods produce short nanotubes in the

0.05–3 μm range, while substrate growth and catalytic gas flow CVD can produce much longer CNTs. The use of fluidized bed CVD is cost effective and results in a high CNT production rate¹⁸. One particularly intriguing fluidized bed CVD process is the CoMoCat technique. This process combines the scalability of fluidized bed reactors with high diameter selectivity²⁴ and is thus attractive where fibers with a specific SWNT diameter are desired.

CNTs that are orders of magnitude longer (from 100 μm up to the centimeter scale) can be produced as vertical arrays by depositing catalyst nanoparticles on a substrate and exposing them to C feedstock gas^{19,21}. Both MWNTs and SWNTs can be produced; SWNT formation is favored by using smaller catalyst particles and a lower C feed rate at the particle surface. Scaling the deposition of catalyst on the substrate seems possible²⁵, although it is still too early to estimate relative complexity and costs. Another method for growing very long nanotubes is catalytic gas flow CVD²². This method can grow millimeter-long nanotubes (a mixture of MWNTs and SWNTs) from a variety of C sources. Depending on the C source, it is possible to control the composition of MWNTs and SWNTs²³. Control of length, control of chirality (particularly for electrical applications) and minimization of defects are the most pressing challenges in the field of CNT synthesis. Along with the scalability of the synthesis process, these challenges are critical for materials applications of CNTs, including the production of neat CNT fibers²⁶.

Formation of CNT fibers

There are two main methods for fiber production: liquid- and solid-state spinning. Natural fibers such as wool and cotton are formed by solid-state spinning (assembling discrete fibers into a yarn), whereas most synthetic fibers are created from a concentrated, viscous liquid. This liquid is a melt or solution of the starting material, which is aligned by flow processing and converted into a fiber through cooling or solvent removal.

Both liquid- and solid-state spinning have been adapted for CNT-based fibers. The development of liquid-state processing has been particularly challenging due to difficulties in processing nanotubes in the liquid state. CNTs do not melt due to their high stiffness and high molecular weight and they are not soluble in organic or aqueous solvents. CNTs tend to form bundles rather than dissolving because of the strong van der Waals forces between their side walls. This is problematic because the nanotubes cannot be controlled and aligned in solution unless they are dispersed at the molecular (single-CNT) level. A number of techniques have been adopted to overcome this problem. CNTs have been functionalized with side groups that make them soluble in common solvents^{25,27}. However, such covalent functionalization destroys their electronic properties and limits the ultimate ordering and packing of the CNTs in the fiber; therefore, this is not a viable option for multifunctional fibers. CNT dispersions can be stabilized in surfactant solution and super-acids; both of these fluid

phases have been used to spin CNT-based fibers. A completely different approach is solid-state spinning, which circumvents the dissolution problem by either drawing a fiber from a vertically grown array of nanotubes or by drawing directly from an aerogel in the furnace. In the following section, both solution- and solid-state spinning will be analyzed.

Surfactant-based solution spinning Dispersion

Surfactants are used to stabilize CNT dispersions because of their ability to form micellar structures around individual CNTs. These CNT/micelle structures are kinetically stable because the surrounding surfactant molecules prevent CNTs from bundling together again.

CNTs are dispersed in an aqueous solution containing a surfactant such as Sodium Dodecyl Sulfate (SDS); the solution is then sonicated to break up CNT bundles and allow the surfactant micelle to encase the CNTs²⁸. The surfactant concentration is critical for the formation of a good dispersion. If it is too low, stabilization is inadequate; if it is too high, the osmotic pressure of the excess micelles causes depletion-induced aggregation. In the case of HiPco SWNTs stabilized by SDS in water, an optically homogeneous solution can be formed with 0.35 wt.% SWNTs and 1 wt.% SDS; however, the exact phase boundaries are a function of SWNT diameter and length. This process has been extended to Double-Walled carbon NanoTubes (DWNTs) and MWNTs^{29,30}, and other surfactants such as Tetra-triMethylammonium Bromide (TMB) and Lithium Dodecyl Sulfate (LDS) have also been used^{31,32}.

Processing and post-processing

Vigolo *et al.*^{33,34} were the first to produce fibers with high SWNT content (above 60 wt.%). In this process, a surfactant-stabilized SWNT solution is coagulated in a PolyVinyl Alcohol (PVA)/water bath; PVA displaces the surfactant and induces flocculation of the SWNTs into an intermediate gel-like fiber structure, termed a 'proto-fiber'. This proto-fiber simultaneously undergoes solvent loss, solidification, stretching and nanotube alignment to form a final solid fiber structure. Some PVA (up to 40%) is retained in the solid fiber and can be removed by post-processing.

The coagulant must flow faster than the proto-fiber in order to promote alignment (Fig. 1b). Vigolo *et al.* accomplished this by rotating the coagulant container (Fig. 1). The method was made continuous and faster by injecting the SWNT dispersion into a cylinder with the coagulant flowing in the same direction^{35,36}.

Coagulation baths other than PVA/water have been utilized in order to produce polymer-free fibers³¹. The coagulants are low-viscosity, polymer-free acids or bases that promote the flocculation of the initial CNT dispersion. Near-instantaneous flocculation occurs with coagulants with $\text{pH} < 1$ or $\text{pH} > 13$. The as-spun fiber retains much of the coagulant (90% liquid content), which can lead to a hollow fiber morphology depending on how the liquid is further removed. Such hollow morphologies show promise for some specialized applications, but fibers spun using these polymer-free coagulants have weak mechanical properties (tensile strength, modulus and toughness) compared with PVA-coagulated fibers³¹. Ethanol/glycerol (1:1 v/v) or ethanol/glycol mixtures (1:3 v/v) can also be used as coagulants for

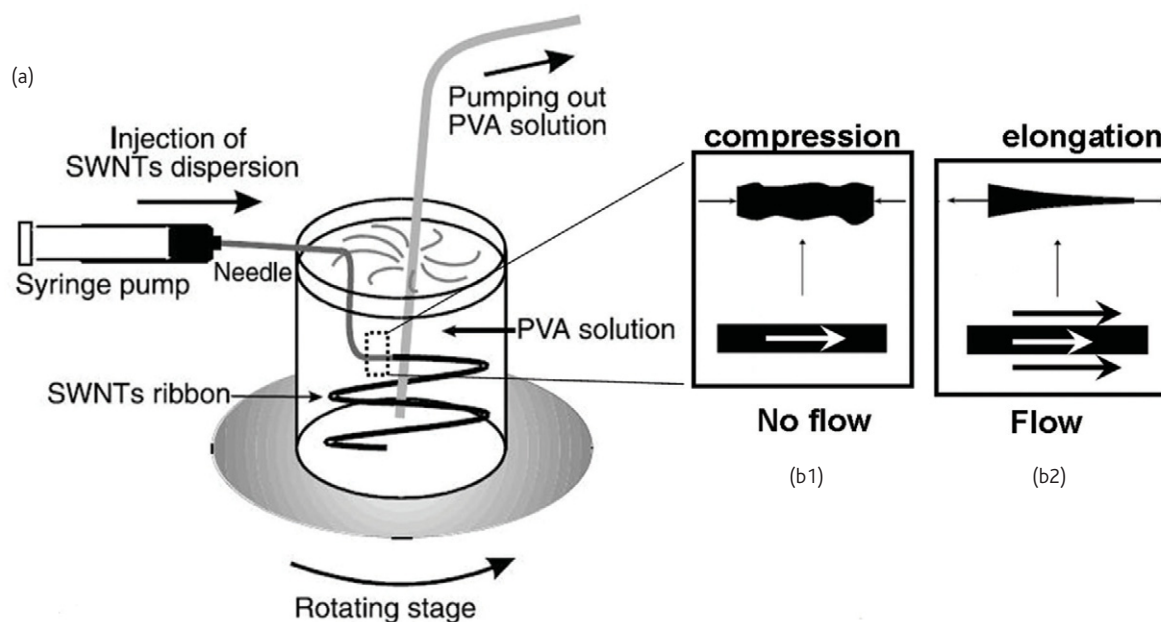


Fig. 1 (a) Schematic of the rotating bath used for coagulating surfactant-dispersed SWNTs into a fiber. When the coagulant bath is not flowed (b1), a net compressive force acts on the proto-fiber, compromising alignment. When the coagulant flows along with the extruded fiber (b2), a net stretching (elongational) force results and increases alignment. (Part (a) is reproduced from Vigolo *et al.*³³. Reprinted with permission from AAAS.)

surfactant-stabilized solution spinning³⁷. The resulting fibers are flexible when wet but become brittle upon drying. Coagulants other than PVA have the advantage of creating polymer-free, electrically conducting fibers; however, the weak mechanical properties of these fibers limit the use of PVA-free coagulants.

Different post-processing treatments have been developed in order to increase SWNT content in the final fiber and to improve mechanical and electrical properties. For example, the fiber can be stretched by swelling it in a PVA solvent and drying it under load³⁴. The fiber does not dissolve in pure PVA solvent, showing that the nanotube–PVA interaction is strong. This technique improves both the Young's modulus (up to 40 GPa) and the tensile strength (up to 230 MPa) of the fiber.

High drawing (5 times the initial length) can also improve fiber properties as shown by Munoz *et al.*³⁶. This is possible because necking behavior, typical of thermoplastic polymer fibers, does not occur. These fibers have high toughness – high tensile strength combined with large failure elongation – and showed the highest energy-to-break (over 600 J/g) ever measured at that time. However, the energy absorbed at low strain was comparatively low; these tough SWNT/PVA fibers absorb an energy of 10 J/g for a strain of up to 10% (for comparison, polyaramide fibers absorb an energy of 35 J/g with up to 3% strain). To improve the low-strain energy absorption, the as-spun fibers are dried and drawn at 850% while being heated at 180°C, i.e. higher than the glass transition, to induce PVA crystallization. The post-processed fiber has a lower strain-to-failure and toughness but absorbs more energy at low strain. The tensile strength increases up to 1.4–1.8 GPa but the maximum strain to failure decreases²⁹.

The load transfer between CNTs and PVA in a PVA/CNT fiber is extremely effective. In fact, the mechanical tensile strength of this fiber is an order of magnitude higher than the fibers coagulated without PVA. However, these fibers do not have a substantially improved modulus and tensile strength compared to pure PVA-made fibers, although they have excellent toughness. Moreover, the presence of the polymer between the CNTs compromises the fibers' electrical properties. The electrical properties can be improved by stretching the as-spun fiber (200 Ω -cm) or by eliminating the polymer by annealing the fiber in hydrogen at 1000°C (0.005 Ω -cm)³⁸.

However, the elimination of PVA is likely to affect the mechanical properties. The PVA coagulation bath technique has also been used for nonsurfactant dispersions of SWNTs. Barisci *et al.*³⁹ dispersed a higher concentration (1 wt.%) of SWNTs in an aqueous DNA solution. The DNA stabilizes the SWNTs by wrapping around the nanotube surface and increasing internanotube repulsion. The resulting fiber properties are inferior to the more recent SDS-based SWNT/PVA fibers. Neri *et al.*⁴⁰ coagulated a basic dispersion (pH 10) of oxidized MWNTs in an acidic (pH 2) PVA (5 wt.%) /water dispersion. Compared with the SDS-based fibers, the resulting fibers had similar toughness and better resistivity, but lower tensile strength and modulus.

Super-acid-based solution spinning Dispersion

Super-acids are the only known solvents for SWNTs^{41,42}. Strong acids such as fuming sulfuric acid are inexpensive solvents that are easily handled industrially; they have been used in the commercial production of high-performance synthetic fibers composed of rod-like polymers⁴³. SWNTs behave as rigid rods when dissolved in super-acids⁴⁴. SWNTs dissolve spontaneously because they are protonated; the ensuing electrostatic repulsion counteracts the attractive van der Waals interactions. The protonation is fully reversible^{41,45}. Depending on the concentration, three distinct regimes are observed. At low concentrations, SWNTs are randomly oriented (isotropic) in the acid. At intermediate concentrations, a biphasic equilibrium between coexisting isotropic and liquid-crystalline phases is observed; higher concentrations result in a fully liquid-crystalline solution (Fig. 2)⁴⁴. The specific phase boundaries are a function of different parameters such as SWNT length^{46,47}, polydispersity^{48,49} and solvent quality⁴⁷.

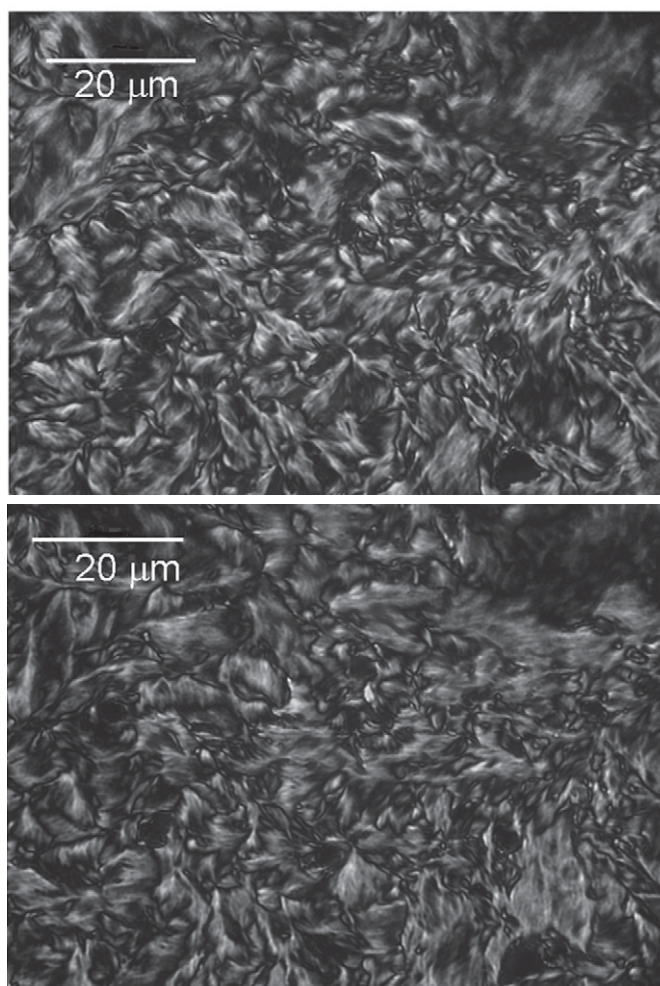


Fig. 2 Microscopy images under cross polars of SWNT (8 wt.%) dissolved in sulfuric acid. Top and bottom images are rotated by 0° and 45°, respectively. The birefringent texture is typical of liquid-crystalline solutions.

Acid solvents have the unique ability to form liquid-crystalline dopes with a high concentration of SWNTs; in sulfuric acid, fibers are spun at 8 wt.% SWNT concentration, over one order of magnitude higher than can be achieved by using surfactants. Because of the spontaneous ordering in the liquid-crystalline phase, these fibers are highly aligned without the need for post-treatments⁵⁰.

Processing and post-processing

Of the possible coagulants for fuming sulfuric acid/SWNT dopes, the use of water or dilute sulfuric acid solutions results in optimum fibers. The density of fibers coagulated in water is 1.11 ± 0.07 g/cm³ (about 77% of a perfectly packed crystal); coagulation in ether yields a low-density (0.87 ± 0.08 g/cm³) dogbone-shaped fiber⁵⁰. The microstructure of the fiber shows large bundles, termed 'super-ropes', 200-600 nm in diameter, and each super-rope is characterized by smaller ropes/bundles with diameters of ~20 nm. These bundles are an order of magnitude larger than bundles observed in the raw material. Thus, the acid process creates a substantial change in the morphology of the initial SWNT powder, although the role of coagulation in the formation of these super-ropes is still poorly understood⁵¹.

A key parameter for improving SWNT alignment and thus fiber properties is the shear rate within the extrusion orifice. For a given extrusion rate, the shear rate scales with orifice diameter cubed. As the diameter is decreased from 500 to 125 μ m, both thermal and electrical conductivity increase because of the increased alignment. The as-spun fiber has a low resistivity due to acid doping, but also has a low modulus. Annealing the fiber in an inert gas at 850°C improves the modulus but simultaneously increases fiber resistivity by an order of magnitude by removing the acid⁵². Spinneret aspect ratios (spinneret length/diameter) used for SWNT/super-acid fiber spinning are usually high (>50) and there is not a clear correlation between fiber alignment and spinneret aspect ratios of 50-200⁵³.

The modulus and electrical properties of acid-spun fibers are among the best values ever reported for CNT-based fibers. However, the tensile strength is low compared to both water/PVA-coagulated fibers and solid-state-drawn CNT fibers. However, this process has not been used for MWNTs or for long (>10 μ m) SWNTs, and if it can be adapted to these longer nanotubes, acid spinning is likely to be the best prospect for scalable spinning of neat CNT fibers.

Solid-state spinning

Naturally occurring fibers include cotton and wool; these materials consist of discrete fibers (diameter 15 μ m, length 3 cm) that can be assembled into a continuous fiber, termed a yarn, by solid-state spinning⁵⁴. Yarn properties improve with increasing fiber length and decreasing fiber diameter²⁰. CNTs have been used in an analogous fashion to produce yarns in a process where individual CNTs or bundles of CNTs act as the constituent fiber in the yarn.

Yarns of CNTs were first observed as discrete fibers formed from CNTs made by gas-phase CVD, 10-20 cm in length and ~5-20 μ m in diameter⁵⁵. These strands had promising electrical resistivity (5 Ω -cm) and tensile strength (0.8 GPa), although not as good as those of individual CNTs. Using the same CVD reaction, Li *et al.*²³ were able to spin the CNT aerogel formed in the reaction zone directly into a continuous fiber.

A different technique was used by Jiang *et al.*⁵⁶; it involves fiber spinning from a vertically grown CNT array and has been used by a number of different research groups^{20,57-59}. Other studies have used solid-state spinning of cotton-like raw material to produce yarns as well^{60,61}.

Synthesis requirements

Not all raw CNT material can be converted into a yarn. For example, Zhang *et al.*²⁰ emphasized bundling within vertically grown CNTs and the disordered regions on the top and bottom of the forests; these disordered regions help to preserve fiber integrity by interlocking the nanotubes. Conversely, studies by Zheng *et al.*⁵⁸ and Li *et al.*²¹ found that highly aligned CNTs that are free of amorphous C are critical for successful solid-state spinning. However, it has been recently shown that it is possible to form fibers from cotton-like, disordered aggregates of nanotubes^{60,61}. These results undermine the notion of prealignment as a key element for solid-state spinning.

For gas-phase CVD solid-state spinning, the C source is the critical factor²³. In fact, CNTs formed from C sources that contain O (i.e. acetone, diethylether) have been successfully spun, while CNTs formed from aromatic hydrocarbons have not. This is likely due to the increased amorphous C associated with aromatic C sources.

In terms of synthesis, other key properties for successful drawing are CNT type (diameter and number of walls) and length. The type and dimension of the catalyst nanoparticles are typically used to control the number of walls, while reaction time controls their length^{21,62}. Motta *et al.*⁶³ argue that large-diameter SWNTs and DWNTs (>5 nm for SWNTs) are particularly desirable because they flatten (buckle radially) into flat sheets, increasing the contact between nanotube surfaces and improving load transfer at the molecular scale. Longer nanotubes have larger surfaces for load transfer and lower fiber defect density (Fig. 3). However, for vertically grown arrays, the growth of longer CNTs comes at the expense of increased amorphous C, which limits the maximum spinnable length. In the gas-phase CVD reaction, a reduced catalyst flow rate results in fibers with improved mechanical properties⁶⁴. This may be due to increased SWNT content, or it may be due to longer nanotubes⁶⁵.

Processing and post-processing

Increases in interbundle contact and density improve the mechanical properties of fibers. A number of different processing

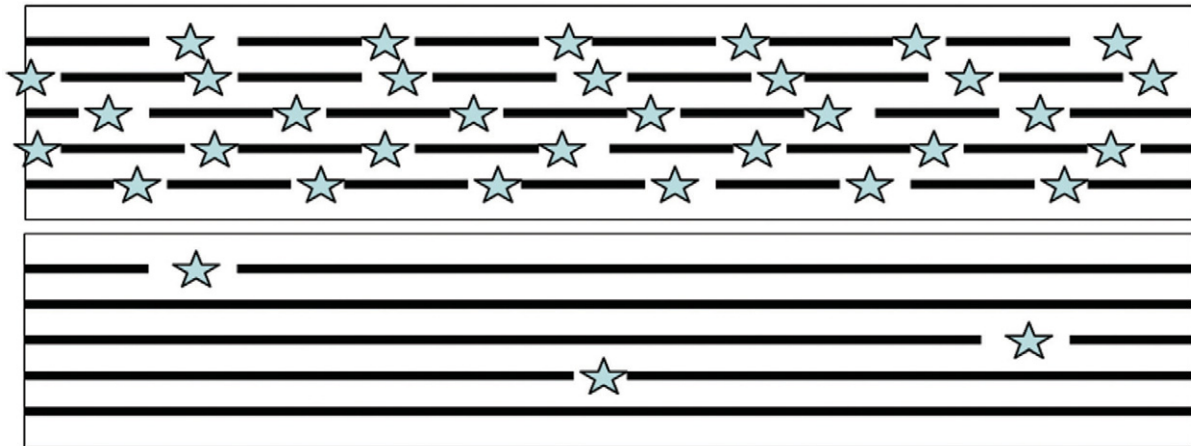


Fig. 3 Schematic depicting two fibers composed of CNTs of different length (top = shorter CNTs; bottom = longer CNTs). The density of end points (indicated by a ☆) between CNTs decreases with growing CNT length. The end point of a nanotube is a defect because the intermolecular interaction between CNTs at the end points is much weaker than the chemical bonds within a single molecule. Decreasing the density of end points should yield fibers with higher tensile strength.

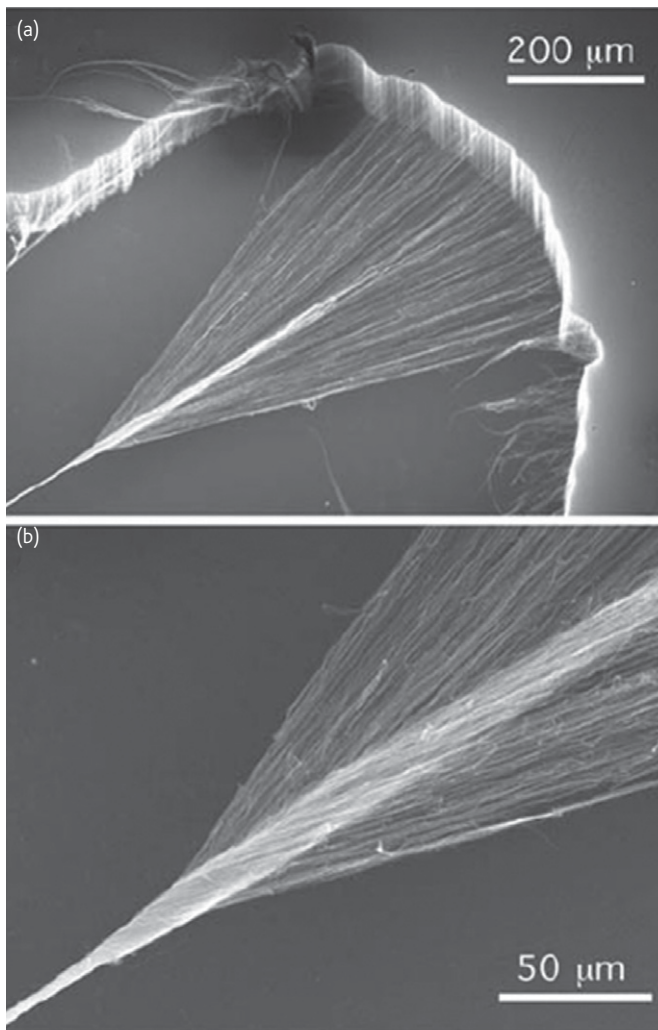


Fig. 4 Scanning electron microscopy images of a carbon nanotube yarn twisted during solid-state spinning. (Reproduced from Zhang *et al.*²⁰. Reprinted with permission from AAAS.)

and post-processing techniques have been used to achieve this goal, including high-speed drawing, twisting and surface-tension-driven densification.

In gas-phase CVD fiber spinning, the CNT-aerogel take-up velocity (winding rate) is a critical parameter: higher winding rates lead to improved alignment and higher density. The maximum achievable winding rate is limited by aerogel breakage.

Twisting is useful because it increases the load transfer between fibers (Fig. 4); it is essential when there are no significant transverse forces to bind the fiber assembly together. Zhang *et al.*²⁰ obtained continuous yarns from relatively short MWNTs (~100 μm) when twisting is applied. The twisted yarn diameter has to be smaller than the length of the constituent CNTs in order for twisting to be effective. Thinner fibers contain a higher fraction of nanotubes with an optimal twist angle. When CNT length is increased, even untwisted yarns are strong enough to be handled and tested⁵⁷.

Surface-tension-driven densification is another technique used to increase fiber density. When fibers spun from vertically grown arrays are pulled through droplets of ethanol, the yarn thickness shrinks by three orders of magnitude⁵⁸. In gas-phase CVD reactions, acetone vapor densification increases yarn density by two orders of magnitude⁶⁶. Ci *et al.*⁶⁰ noted that the starting, cotton-like material must be wet in order to draw a continuous fiber because the wet material is denser and has stronger internanotube interactions. Solid-state drawn fibers are usually flexible. Zhang *et al.*⁵⁸ attribute this property to the small diameter of such fibers and weak intertube bonding, which results in smaller bending stresses. Flexible fibers reported so far usually have low fiber modulus^{20,58}. However, thermal annealing can reduce this flexibility and increase fiber modulus⁵⁸; thus, thermal annealing of flexible fibers can be used to lock the geometry of a given shape⁵⁸. This can be explained by the fact that nanotubes tend to create covalent bonds at high temperature by 'welding' to each other^{67,68}.

Another useful post-processing technique is infiltration by a polymer solution such as PVA, which can double fiber strength²⁰. Unlike coagulation in water/PVA, this technique does not dramatically compromise the electrical properties of fibers because PVA fills up voids and improves internanotube load transfer without compromising internanotube connectivity. This technique is particularly effective for porous fibers, including most solid-state drawn fibers.

The mechanical and electrical properties of solid-state drawn fibers are limited because of their porous morphology. Typical fiber

morphology involves three levels of organization. The constitutive macromolecules are CNTs and the next level involves CNT bundles with typical diameters of 20-60 nm, which are much smaller than the 'super ropes' obtained via the super-acid process. The microstructure level consists of a loosely connected bundle network with a preferred orientation along the fiber axis. The density of these fibers is only 30–50% of the perfect nanotube packing density even after densification post-treatment. This indicates that the effectiveness of the various post-processing techniques is

Table 1 CNT fiber properties for both solution and solid-state spinning from the main articles published to date.

| Solution spinning | | | | | | | | | | |
|--|------|---------------------|---------------------|-----------------|--------------------|-----------------------|------------------------|-----------------------|---------------------------------------|------------------------------|
| Spinning technique | ref. | CNT characteristics | | | Comments | Mechanical Properties | | | Electrical resistivity (mΩ·cm) | Thermal conductivity (W/m·K) |
| | | Type | Length (μm) | diameter (nm) | | Modulus (GPa) | Strength (GPa) | Toughness (J/g) | | |
| Surfactant dispersion coagulated in water-PVA | [33] | | | | as-spun | 15 | 0.15 | 2.25 ^c | | |
| | [34] | | | | stretched | 40 | 0.23 | 0.82 ^c | | |
| | [38] | | | | annealed | – | – | – | 10 | 10 |
| | [35] | | | | stretched | 80 | 1.8 | 570 | | |
| Surfactant dispersion coagulated in ethanol/glycerol | [37] | SWNT | sub μm ^e | ~1 ^e | as-spun | 2 | weak | – | 150 | – |
| Surfactant dispersion coagulated in acid or base | [31] | | | | as-spun | 12 | 0.065 | – | 150 | – |
| Sulfuric acid dispersion coagulated in water | [50] | | | | annealed | 120 | 0.116 | – | 0.2 | 20 |
| Solid-state spinning | | | | | | | | | | |
| Gas-phase CVD | [23] | MWNT | ~30 | 30 | as-spun | – | 0.1-1 | – | 2.5 ^x (0.12 ⁱ) | – |
| | [66] | DWNT | ~1000 | 10 | vapor condensed | 78(160 ^y) | 1.3(5.9 ^y) | 13(116 ^y) | – | – |
| Vertical-grown CNT array spinning | [20] | MWNT | 100 | 10 | twisted | 5-30 | 0.15-0.46 | 11-20 | 3.3 | – |
| | [73] | | | | | | | | | 26 |
| | [58] | MWNT | – | 5-15 | methanol condensed | 37 | 0.6 | 13 | – | – |
| | [62] | MWNT | 650 | 10 | un-twisted | 275 | 0.85 | – | 5.8 | – |
| | | | | | twisted | 330 | 1.91 | – | 2.4 | – |
| [57] | DWNT | 1000 | 7 | twisted | 100-263 | 1.35-3.3 | 110-974 | 1.68 | – | |
| Cotton-like spinning | [61] | MWNT | >1000 | ~250 | twisted | 180 ^c | 0.19 ^c | – | – | – |
| | [60] | DWNT | – | 1-2 | twisted while wet | 8.3 | 0.299 | – | – | – |

^c = calculated using information within the paper

^e = estimated from Carver *et al.*⁶⁵

ⁱ = based on graphite density

^x = extrapolated based on typical fiber density

^y = tensile strength performed on 1 mm gauge length with a best value of 8.8 GPa

limited and solid-state drawn fibers inherently suffer from porous morphology.

Fiber properties

CNTs' unique combination of mechanical, thermal and electrical properties makes CNT-based fibers perfect candidates for multifunctional materials. In the following section, we review the theoretical limits for the properties of a macroscopic assembly and compare these with actual experimental values (Table 1).

Mechanical properties

Although the tensile strength of individual nanotubes is very high, the properties of a macroscopic assembly of aligned nanotubes are dictated by the strength of the constituent bundles (or ropes) and their connectivity. Even when single nanotubes are perfectly aligned into a single bundle, the failure of this assembly can occur via the slippage of the constitutive CNTs at a stress lower than the failure stress of the single molecule⁶⁹. Three main forces are involved in maintaining bundle integrity: intrinsic nanotube strength, capillary forces (energy required to form a free surface) and internanotube friction⁶⁹. Depending on the aspect ratio, three regions can be distinguished (Fig. 5). At low aspect ratios, capillary forces dominate and the failure strength is independent of the aspect ratio. At intermediate aspect ratios, the failure strength depends on internanotube friction and is linearly proportional to the length. At high aspect ratios, the fiber tensile strength is equal to that of the individual nanotubes.

A plot of measured tensile strength of neat CNT fibers vs. CNT aspect ratio confirms that tensile strength increases with aspect ratio

(Fig. 6). Yakobson *et al.*⁶⁹ estimate a SWNT length of 10 μm (1 nm diameter) for a perfectly packed fiber to attain the potential failure strength of an individual SWNT. So far, even fibers produced from millimeter-long nanotubes^{57,66} show a tensile strength that is nearly two orders of magnitude lower than the breaking stress on a single CNT; this is most likely due to poor alignment and packing of the CNTs in the constitutive bundle and/or low interbundle connectivity.

The theoretical linear relationship between strength and aspect ratio should generally hold for experimental fibers with imperfect morphology. (This is readily seen in the three fibers from Zhang *et al.*⁶² in Fig. 6.) Fibers with this line shifted to the left have a better morphology. In fact, if liquid-state morphology (alignment and packing) can be obtained with longer constitutive nanotubes, this can lead to fibers with better tensile strength.

Koziol *et al.*⁶⁶ emphasize the effect of fiber 'weak points' on tensile strength measurements. Tensile strength is low if these weak points occur within the gauge length, while testing portion of fibers without weak points can give an idea of the true potential of the material. In gas-phase CVD fiber spinning, tensile strength can be increased by almost an order of magnitude depending on the gauge length used for the measurements⁶⁶.

The CNT-based fiber moduli reported thus far are 1–2 orders of magnitude lower than what is theoretically attainable and it seems that there is not yet a clear correlation between modulus and CNT aspect ratio (Fig. 7a). This strongly contrasts with rod-like polymer fibers, where commercial fiber moduli have actually matched the theoretical crystal modulus⁷⁰. An exception to this is the modulus of 263 GPa reported by Zhang *et al.*⁵⁷; however, the specific modulus (modulus/

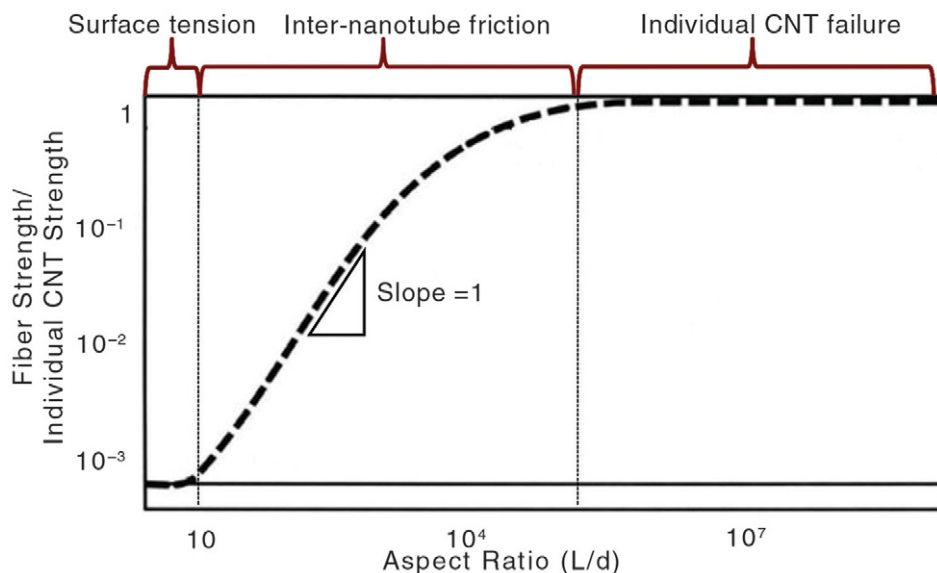


Fig. 5 Tensile strength of a perfectly aligned bundle of CNTs as a function of aspect ratio. Three regions can be distinguished. The first is dominated by capillary forces and is independent of aspect ratio. The intermediate region is dominated by internanotube friction and tensile strength is linearly proportional to CNT aspect ratio (slope of 1 in a log–log plot). In the final region (at higher aspect ratios), bundle tensile strength coincides with the strength of a single CNT. (Reproduced with permission from Yakobson *et al.*⁶⁹.)

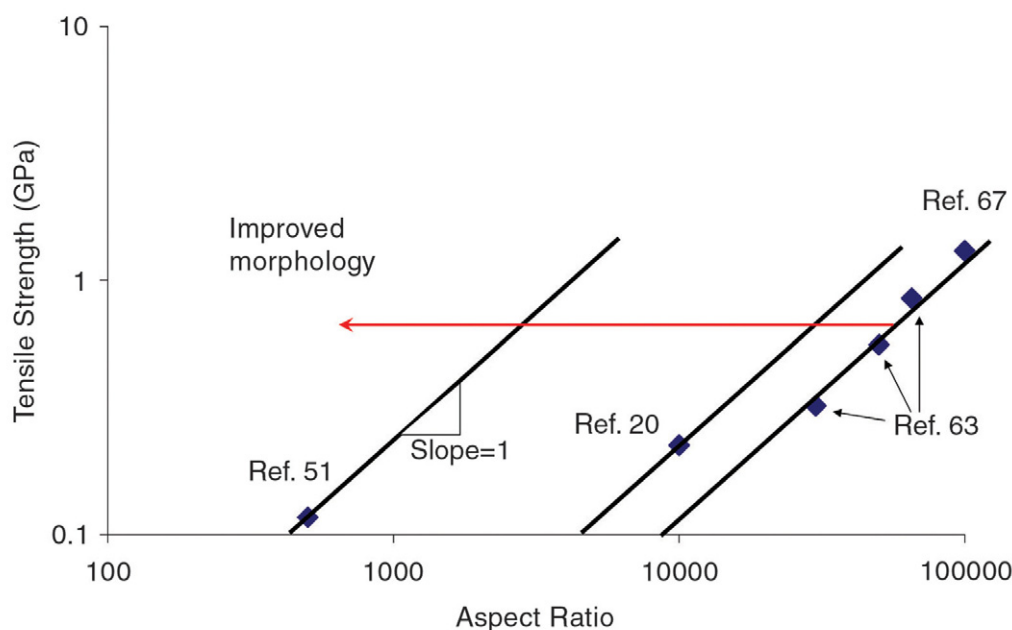


Fig. 6 Tensile strength of different CNT fibers as a function of the aspect ratio. A slope of 1 has been drawn through each data point to indicate how the tensile strength of these fibers will scale with CNT length. This allows the morphology of the fibers to be compared independently of the aspect ratio of the constituent CNTs.

density) of this fiber is slightly higher than what is theoretically achievable. This inconsistency could be due to higher single-molecule properties in this specific case; however, further elucidation is needed from the authors to explain this apparent contradiction.

SWNT–PVA composite fibers have exhibited the highest toughness attained so far, although the low-strain energy absorption is comparatively low. Some of the solid-state drawn CNT fibers show very high toughness as well (maximum 975 J/g, average 309 J/g)⁵⁷. These high values of toughness are related to the nonbrittle behavior of these fibers. In fact, these fibers do not fracture at the highest stress; instead they yield gradually until they finally break.

Electrical and thermal properties

Individual CNTs exhibit excellent thermal and electrical properties. The current-carrying capacity of metallic nanotubes can be 1000 times better than that of Cu⁷¹ and the thermal conductivity of CNTs can be higher than 3000 W/m-K⁸. However, lattice defects such as vacancies, substitutions, pentagon–heptagon defects and chirality mismatches within a nanotube can decrease the conductivity. These defects are more common in long CNTs. Currently, there are no production or separation methods that can yield bulk quantities (milligram or larger) of metallic nanotubes.

Other reasons for decreased conductivity (both thermal and electrical) of a macroscopic assembly are related to nanotube length and alignment. The resistance is the sum of intrinsic nanotube resistance and internanotube contact. In Zhang *et al.*⁵⁷ the measured fiber density is 0.195 g/cm³; hence the specific modulus becomes 1282 GPa/SG, from dividing the single-molecule modulus (1 TPa)

by the single-molecule density 0.78 (reported by the authors in the supplementary information). The contact density can be lowered with longer, better aligned nanotubes. The comparison between electrical conductivity of neat SWNT fibers with varying aspect ratios does not yet show this clear trend (Fig. 7b). In fact, acid-spun fibers show very low resistivity (0.2 Ω-cm) when acid doped and they maintain relatively low resistivity even upon annealing (2.62 Ω-cm). Even after annealing, the resistivity of acid-spun fibers is lower than that of most solid-state drawn fibers²⁰. This is counterintuitive, because acid-spun fibers consist of shorter SWNTs (<1 μm) and it may stem from several different causes. First, in acid-spun fibers the CNTs coalesce into more regular ropes than in solid-state drawn fibers. Second, HiPco SWNTs used for acid spinning have fewer defects than array-grown ultra-long MWNTs. The resistivity of solid-state drawn fibers decreases as the aspect ratio increases⁷²; nevertheless, the resistivity difference between acid-spun and solid-state drawn fibers shows the importance of good coalescence as a means to improve properties. In current fiber production methods, the degree of coalescence controls resistivity more than aspect ratio does.

Few data have been reported for the thermal conductivity of CNT-based fibers. 20 W/m-K was reported for acid spun fibers, while annealed PVA/water spun fibers have half this value. Solid-state drawn yarns have a slightly better value of 26 W/m-K⁷³; however, these values are two orders of magnitude lower than the thermal conductivity of K-1100, a commercial carbon fiber⁷⁴. Further advances in thermal and electrical conductivity should track each other because both aspects are ultimately controlled by related physical mechanisms⁷⁵.

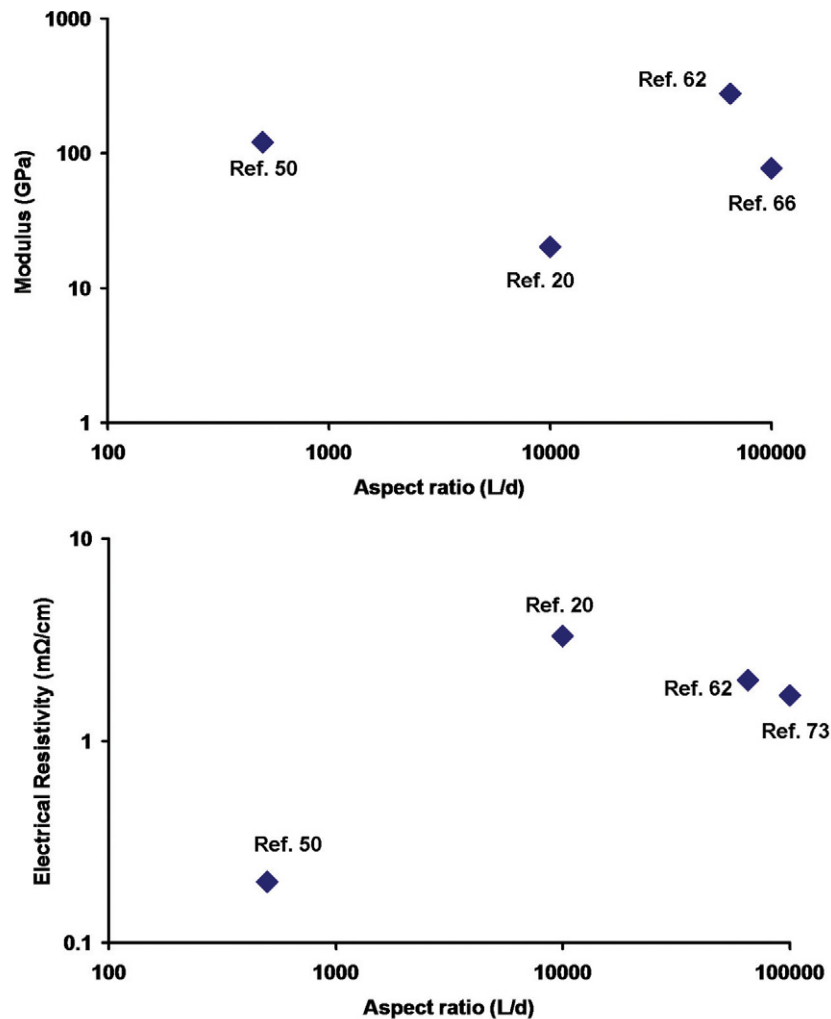


Fig. 7 Modulus and electrical resistivity of different CNT fibers as a function of the CNT aspect ratio. (a) Fiber modulus does not increase monotonically with respect to the aspect ratio as tensile strength does. (b) Electrical resistivity does not change substantially with CNT aspect ratio. For solid-state drawn fibers, electrical resistivity decreases with aspect ratio; acid-spun fibers are an exception to this trend. The data can have significant scatter for a given aspect ratio depending on processing and/or post-processing. Average data were used when available.

Future directions

The property of fibers of CNTs are still far from those of their constituent elements. Further improvements will result from improved control in CNT production and improved fiber processing and/or post-processing. For example, effective coalescence has been demonstrated in solution spinning and post-processing has improved the tensile strength of the original CNT-based fibers by an order of magnitude. However, in contrast to solid-state spinning, solution-spinning methods have not yet been used to successfully process long CNTs. The mechanical properties of these solid-state drawn fibers have been improved by an order of magnitude through the use of longer nanotubes as well as post-processing techniques such as twisting and liquid or vapor condensation. However, even millimeter-long nanotubes have not yet matched what is theoretically achievable due to the poor coalescence observed in solid-state spinning.

These same fiber qualities are also required for improved thermal and electrical properties, although coalescence appears to be the critical factor for thermal and electrical properties, whereas CNT aspect ratio is critical for mechanical properties. One challenge specific to electronic applications is the production and/or separation of specific SWNT chiralities. Current SWNT synthesis methods produce a mixture of either metallic or semiconducting SWNTs, but unfortunately no separation techniques have yet demonstrated the ability to effectively separate bulk quantities.

Conclusions

In the last decade, a number of different techniques for CNT-based fiber assembly have emerged. Specifically, there are two main types of processes by which CNTs fibers can be assembled. The first is solution spinning, where the nanotubes are dispersed in surfactant or

solubilized in acid and then coagulated into a fiber. The second is solid-state spinning, where fibers are drawn from a vertically grown array of nanotubes or directly collected from the aerogel formed in the reaction furnace. Solution spinning is readily scalable but has not yet shown the ability to process long nanotubes. Solid-state spinning has exhibited the best mechanical properties for CNT fibers to date. However, the process scalability and fiber morphology are problematic.

Future developments in CNT-based fibers will stem from two areas: improvements in the starting material (i.e. longer, defect-free, type-specific CNTs), or improvements in the processing and post-processing of the fibers. Given the wide range of achievements in CNT synthesis and fiber processing of the past decade, the prospect of high-performance CNT-based fibers is quite promising, particularly

as researchers continue to apply the effective techniques of rigid-rod polymer processing to SWNT fibers. **nl**

Acknowledgments

The authors wish to thank Wade Adams, Robert Hauge, Howard Schmidt, Satish Kumar, Wen-Fang Hwang, Karla Strong, Benji Maruyama, Cary Pint, Nicholas Parra-Vasquez, Colin Young and Richard Booker for their helpful input. This work was funded by AFOSR grant FA9550-06-1-0207, QWD grant 07-S568-0042-01-C1, and an Evans-Attwell Welch Postdoctoral Fellowship. This material is based on research sponsored by Air Force Research Laboratory under agreement number FA8650-07-2-5061. The U. S. Government is authorized to reproduce and distribute reprints for Governmental Purposes notwithstanding any copyright notation thereon. The views and conclusions contained herein are those of the authors and should not be interpreted as necessarily representing the official policies or endorsements, either expressed or implied, of AFRL or the U. S. Government.

References

- Adams, W. W., et al., *The Materials Science and Engineering of Rigid-Rod Polymers*, Materials Research Society, Warrendale, PA, (1989), vol. 134.
- Treacy, M. M. J., et al., *Nature* (1996) **381**, 678.
- Pasquali, M., et al., *Phys. Rev. Lett.* (2006) **96**, 246104.
- Yakobson, B. I., et al., *Carbon Nanotubes* (2001) **80**, 287.
- Yamamoto, T., et al., *Carbon Nanotubes* (2008) **111**, 165.
- Tans, S. J., et al., *Nature* (1997) **386**, 474.
- Hone, J., et al., *Appl. Phys. Lett.* (2000) **77**, 666.
- Baughman, R. H., et al., *Science* (2002) **297**, 787.
- Iijima, S., *Nature* (1991) **354**, 56.
- Ebbesen, T.W., et al., *Nature* (1992) **358**, 220.
- Bethune, D. S., et al., *Nature* (1993) **363**, 605.
- Kroto, H. W., *Nature* (1985) **318**, 162.
- Guo, T., *Chem. Phys. Lett.* (1995) **243**, 49.
- Thess, A., et al., *Science* (1996) **273**, 483.
- Arepalli, S., *J. Nanosci. Nanotechnol.* (2004) **4**, 317.
- Pavel, N., *J. Nanosci. Nanotechnol.* (2004) **4**, 307.
- Dai, H. J., et al., *J. Phys. Chem. B* (1999) **103**, 11246.
- See, C. H., et al., *Ind. Eng. Chem. Res.* (2007) **46**, 997.
- Fan, S. S., et al., *Science* (1999) **283**, 512.
- Zhang, M., et al., *Science* (2004) **306**, 1358.
- Li, Q. W., et al., *Adv. Mater.* (2006) **18**, 3160.
- Li, Y. L., et al., *Nanotechnology* (2007) **18**, 22.
- Li, Y. L., et al., *Science* (2004) **304**, 276.
- Resasco, D. E., *J. Nanoparticle Res.* (2002) **4**, 131.
- Nishino, H., et al., *J. Phys. Chem. C* (2007) **111**, 17961.
- Joselevich, E., et al., *Carbon Nanotubes*, Springer-Verlag, Berlin, (2008), 101.
- Liang, F., et al., *Nano Lett.* (2004) **4**, 1257.
- O'Connell, M. J., et al., *Science* (2002) **297**, 593.
- Miaudet, P., et al., *Nano Lett.* (2005) **5**, 2212.
- Razal, J. M., et al., *Adv. Funct. Mater.* (2007) **17**, 2918.
- Kozlov, M. E., et al., *Adv. Mater.* (2005) **17**, 614.
- Poulin, P., et al., *Carbon* (2002) **40**, 1741.
- Vigolo, B., *Science* (2000) **290**, 1331.
- Vigolo, B., et al., *Appl. Phys. Lett.* (2002) **81**, 1210.
- Dalton, A. B., et al., *Nature* (2003) **423**, 703.
- Munoz, E., et al., *Adv. Eng. Mater.* (2004) **6**, 801.
- Steinmetz, J., et al., *Carbon* (2005) **43**, 2397.
- Badaire, S., *J. Appl. Phys.* (2004) **96**, 7509.
- Barisci, J. N., et al., *Adv. Funct. Mater.* (2004) **14**, 133.
- Neri, W., et al., *Macromol. Rapid Commun.* (2006) **27**, 1035.
- Ramesh, S., et al., *J. Phys. Chem. B* (2004) **108**, 8794.
- Rai, P. K., *J. Am. Chem. Soc.* (2006) **128**, 591.
- Choe, E. W., and Kim, S. N., *Macromolecules* (1981) **14**, 920.
- Davis, V. A., et al., *Macromolecules* (2004) **37**, 154.
- Engtrakul, C., *J. Am. Chem. Soc.* (2005) **127**, 17548.
- Onsager, L., *Ann. N.Y. Acad. Sci.* (1949) **51**, 627.
- Flory, P. J., *Proc. R. Soc Lond. A* (1956) **234**, 73.
- Flory, P. J., et al., *Macromolecules* (1978) **11**, 1126.
- Odijk, T., et al., *J. Phys. Chem.* (1985) **89**, 2090.
- Ericson, L. M., et al., *Science* (2004) **305**, 1447.
- Fan, H., Wet-spinning of Neat Single-walled Carbon Nanotube Fiber from 100+% H₂SO₄, PhD thesis, Rice University, Houston, TX, 2007.
- Zhou, W., et al., *J. Appl. Phys.* (2004) **95**, 649.
- Ericson, L. M., Macroscopic Neat Single-wall Carbon Nanotube Fibers, PhD thesis, Rice University, Houston, TX, 2003, fig. 3.25, p. 101.
- Morton, W. E., and Hearle, W. S., *Physical Properties of Textile Fibres*, Butterworth, London, 1962.
- Zhu, H. W., et al., *Science* (2002) **296**, 884.
- Jiang, K. L., *Nature* (2002) **419**, 801.
- Zhang, X. F., *Adv. Mater.* (2007) **19**, 4198.
- Zhang, X. B., et al., *Adv. Mater.* (2006) **18**, 1505.
- Zhang, S., *J. Mater. Sci.* (2008) **43**, 4356.
- Ci, L., et al., *Adv. Mater.* (2007) **19**, 1719.
- Zheng, L. X., et al., *Adv. Mater.* (2007) **19**, 2567.
- Zhang, X. F., et al., *Small* (2007) **3**, 244.
- Motta, M., et al., *Adv. Mater.* (2007) **19**, 3721.
- Motta, M., *Nano Lett.* (2005) **5**, 1529.
- Carver, R. L., et al., *J. Nanosci. Nanotechnol.* (2005) **5**, 1035.
- Koziol, K., et al., *Science* (2007) **318**, 1892.
- Kim, Y., *Chem. Phys. Lett.* (2004) **398**, 87.
- Fantini, C., et al., *Phys. Rev. B* (2006) **73**, 193408.
- Yakobson, B. I., et al., *Carbon* (2000) **38**, 1675.
- Chae, H. G., et al., *Appl. Polym. Sci.* (2006) **100**, 791.
- Szleifer, I., et al., *Polymer* (2005) **46**, 7803.
- Li, Q. W., et al., *Adv. Mater.* (2007) **19**, 2567.
- Aliev, A. E., et al., *Carbon* (2007) **45**, 2880.
- Minus, M. L., et al., *JOM* (2005) **57**, 52.
- Lavin, J. G., et al., *Carbon* (1993) **31**, 1001.